Mapana - Journal of Sciences
2021, Vol. 20, No. 2, 27-58
ISSN 0975-3303 | https://doi.org/10.12723/mjs.57.3

Influence of Heat Generation and Thermal Radiation on MHD Flow in a Vertical Micro-Porous-Channel in the Presence of Viscous Dissipation

Ponna Bhaskar* and Malapati Venkateswarlu†

Abstract

This article analyses the influence of heat generation and thermal radiation on steady hydromagnetic fully developed natural convection flow in a vertical micro-porous–channel in the presence of viscous dissipation. The governing ordinary differential equations, exhibiting the physics of the flow formation are displayed. Using the relevant non–dimensional variables, the governing equations are transformed into their corresponding non–dimensional form and then solved exactly by employing the perturbation technique. The influence of different admissible parameters such as fluid wall interaction parameter, Knudsen number, heat generation parameter, thermal radiation parameter, magnetic parameter, Eckert number, and permeability parameter on the fluid velocity, temperature, skin friction coefficient, and heat transfer coefficient at the micro-porous–channel surfaces is discussed with the aid of line graphs and tables.

Keywords: Hydromagnetic, wall ambient temperature ratio, velocity slip, temperature jump

* Department of Mathematics, Shri Venkateshwara University, Rajabpur Gajraula, U.P., India; ponnabhaskar75@gmail.com
† Department of Mathematics, V. R. Siddhartha Engineering College, Vijayawada, A.P., India; mvsr2010@gmail.com

Nomenclature

a – Distance between two parallel plates

B_0 - Uniform magnetic field

C_f - Skin-friction coefficient

c_p - Specific heat at constant pressure

c_v - Specific heat at constant volume

F_v - Momentum accommodation coefficient

F_t - Thermal accommodation coefficient

g – Acceleration due to gravity

k_T - Thermal conductivity of the fluid

kn – Knudsen Number

ln – Fluid wall interaction parameter

M – Magnetic parameter

Nu – Nusselt number

Pr – Prandtl number

Q_0 - Dimensional heat generation parameter

q_w – Heat flux

Re – Reynolds number

H – Heat generation parameter

T – Fluid temperature

T_0 - Reference temperature

T_1 - Hot wall temperature

T_2 - Cold Wall temperature

U – Non-dimensional velocity

u_0 - Mean velocity

u – Fluid velocity in x - direction

ν – Fluid velocity in y - direction

Greek Symbols

β_T - Coefficient of thermal expansion

ν – Kinematic coefficient of viscosity

ρ – Fluid density

σ – Fluid electrical conductivity σ – Fluid electrical conductivity

τ_w - Shear stress

α – Thermal diffusivity of the fluid

γ– Ratio of specific heats

λ – Molecular mean free path

β_v, β_t - Non-dimensional variables

ξ – Wall ambient temperature

η – A scaled coordinate

θ – A scaled temperature

1. Introduction

The irreversible process through which the work done by a fluid on adjacent layers due to the action of shear forces is transformed into heat is defined as viscous dissipation. Viscous dissipation is of interest for several applications, significant temperature rises are observed in polymer processing flows such as injection moulding or extrusion at high rates. The influence of viscous dissipation on heat transfer is important, especially for highly viscous flows even with moderate velocities. Viscous dissipation transforms the kinetic energy to internal energy (heating up the fluid) due to viscosity and hence increases the fluid motion. Given this reason, various devices are designed in streambeds to reduce the kinetic energy of flowing water to reducing their erosive potential on banks and river bottoms. Due to this, the non-dimensional parameter Eckert number is called the fluid motion controlling parameter. Ali et al. presented the numerical simulation of flow and heat transfer in the hydromagnetic micro-polar fluid between two stretchable disks with viscous dissipation effects. Altunkaya et al. discussed the effects of viscous dissipation on mixed convection in a vertical parallel plate micro-channel with asymmetric uniform wall heat fluxes. Gnaneswara Reddy et al. studied the effects of viscous dissipation and heat source on unsteady MHD flow over a stretching sheet. Anjali and Ganga considered the effects of viscous and joules dissipation on MHD flow, heat and mass transfer past a stretching porous surface embedded in a porous medium. Jha and Aina presented the impact of viscous dissipation on fully developed natural convection flow in a vertical microchannel. Venkateswarlu et al. investigated the effects of chemical reaction and heat generation on MHD boundary layer flow of a moving vertical plate with suction and dissipation. Barletta studied the laminar mixed convection with viscous dissipation in a vertical channel. Prasad et al. presented the mixed convective fully developed flow in a vertical channel in the presence of thermal radiation and viscous dissipation. Umavathi et al. discussed the combined effect of variable viscosity and thermal conductivity on the free convection flow of a viscous fluid in a vertical channel.

Micro-channel fluid mechanics have attracted important research interest in recent years due to the rapid growth of novel techniques

applied in micro-electro-mechanical systems, manufacturing, material processing operations, space systems and biomedical applications such as drug delivery, DNA sequencing, bio-micro-electro-mechanical systems. The present development of automotive, aerospace and electronic technologies has been connected with a reduction in the size of components and an increase in their power and heat generation. Several theoretical investigations have been carried out on micro-scale convection for slip flow in the past decade. Jha et al. presented the MHD natural vertical parallel plate micro-channel. Buonomo and Manca discussed the natural convection flow in a vertical microchannel heated at uniform heat flux. Aydin and Avci investigated the thermally developing flow in micro-channels. Chen and Weng studied the natural convection in a study of convective heat transfer in silicon micro-channels with different surface conditions. Haddad et al. considered the developing free-convection gas flow in a vertical open-ended micro-channel filled with porous media. Venkateswarlu et al. presented the influence of thermal radiation and heat generation on steady hydromagnetic flow in a vertical micro-porous-channel in presence of suction/injection. Jha and Aina discussed the mixed convection flow in a vertical micro-annulus having temperature-dependent viscosity. Khadrawi et al. studied the transient free convection fluid flow in vertical micro-channels described by the hyperbolic heat conduction model. Wu and Cheng presented an experimental convection flow in a vertical parallel plate micro-channel. Jha et al. discussed the natural convection flow in a vertical micro-channel with suction/injection.

The study of hydromagnetic flows has stimulated considerable interest due to its significant physical applications in solar physics, power generating systems, meteorology, cosmic fluid dynamics, aeronautics, missile aerodynamics and the motion of Earth's core (see, Cramer & Pai and Sparrow & Cess). In a broader sense, MHD has applications in three different subject areas, such as engineering, astrophysical and geophysical problems. In light of these applications, Hayat et al. presented the mixed convection flow of a micro-polar fluid with radiation and chemical reaction. Venkateswarlu and Makinde discussed the unsteady MHD slip flow with radiative heat and mass transfer over an inclined plate embedded in a porous medium. Kataria and Patel studied the

radiation and chemical reaction effects on MHD Casson fluid flow past an oscillating vertical plate embedded in a porous medium. Malapati and Dasari considered the Soret and chemical reaction effects on the radiative MHD flow from an infinite vertical plate. Seth, et al. presented the hydromagnetic natural convection flow with heat and mass transfer of a chemically reacting and heat-absorbing fluid past an accelerated moving vertical plate with ramped temperature and ramped surface concentration through a porous medium. Adhikary and Misra discussed the unsteady two-dimensional hydromagnetic flow and heat transfer and heat transfer of fluid. Garg et al. investigated the oscillatory MHD convective flow of second-order fluid through a porous medium in a vertical rotating channel in a slip-flow regime with heat radiation.

Heat transfer and MHD flows in porous media have been studied extensively in recent years due to their occurrence in several engineering processes such as compact heat exchangers, casting, filtration of liquid metals, metallurgy, cooling of nuclear reactors and fusion control. Jha and Aina presented the mathematical modelling and exact solution of steady fully developed mixed convection flow in a vertical micro-porous-annulus. Venkateswarlu et al. studied the Dufour and heat source effects on radiative MHD slip flow of a viscous fluid in a parallel porous plate channel in presence of a chemical reaction. Seth et al. discussed the unsteady hydromagnetic natural convection flow of heat-absorbing fluid within a rotating vertical channel in a porous medium with Hall Effect. Venkateswarlu et al. presented the influence of slip condition on radiative MHD flow of a viscous fluid in a parallel porous plate channel in presence of heat absorption and chemical reaction. Seth et al. considered the unsteady MHD convective flow within a parallel plate rotating channel with thermal source/sink in a porous medium under slip boundary conditions. Adesanya and Makinde studied the MHD oscillatory slip flow and heat transfer in a channel filled with porous media.

The objective of the present study is to extend the work of Jha and Aina by introducing the influence of magnetic parameter, permeability parameter in the momentum equation and radiation parameter, heat generation parameter in the energy equation. We should in prior emphasize that our intention is not to reproduce the

results of Jha and Aina. Analytical closed-form expressions are produced for momentum and energy equations using some proper change of variables. The following strategy is pursued in the rest of the paper. Section two presents the formation of the problem. The analytical expressions are presented in section three. Results are discussed in section four and finally, section five provides a conclusion of the paper.

2. Formulation of the Problem

Consider the fully developed steady hydromagnetic flow of a viscous, incompressible and electrically conducting fluid in a micro-porous–channel between two parallel plates as shown in Fig. 1. The distance between two parallel plates is a. A Cartesian coordinate system is selected such that $x-$axis is parallel to the gravitational acceleration g and $y-$axis is normal to the channel walls. A uniform magnetic field of strength B_0 is applied normal to the parallel plates. Thermal radiation and heat generation parameters are taken into consideration. The micro-channel plates are heated asymmetrically with one plate maintained at a temperature T_1 while the other plate at a temperature T_2 with $T_1 > T_2$. In addition, fluid is being injected into the flow region through the cold porous plate and to conserve the mass of the fluid in the micro-porous–channel, fluid is being sucked out of the micro-porous–channel at the same rate through the hot porous plate. It is assumed that the fluid has constant physical properties. Using Boussinesq's approximation, the dimensional governing equations of the continuity, momentum and energy can be written as follows (see, Jha and Aina):

Continuity equation:

$$\frac{dv}{dy} = 0 \tag{1}$$

Momentum equation:

$$\nu \frac{d^2u}{dy^2} - \frac{\sigma B_0^2}{\rho} u + g\beta_T \left(T - T_0\right) - \frac{\nu}{K_1} u = 0 \tag{2}$$

Energy equation:

$$\alpha \frac{d^2T}{dy^2} + \frac{Q_0}{\rho c_p}\left(T - T_0\right) + \frac{\nu}{c_p}\left[\frac{du}{dy}\right]^2 - \frac{1}{\rho c_p}\frac{\partial q_r}{\partial y} = 0 \tag{3}$$

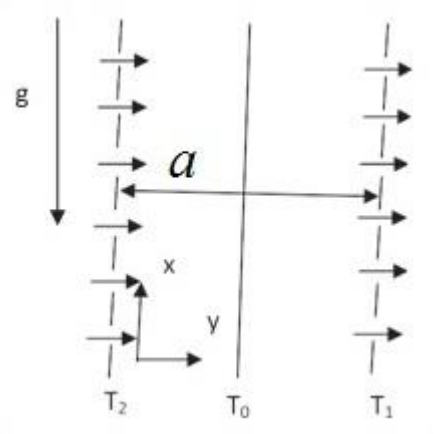

Fig.1: Geometry of the problem.

Here u – fluid velocity in x – direction, v – fluid velocity in y – direction, B_0 – uniform magnetic field, ρ – fluid density, ν – the kinematic viscosity of the fluid, σ – fluid electrical conductivity, g – gravitational acceleration, β_T – thermal expansion coefficient, T – fluid temperature, T_0 – reference temperature, K_1 – dimensional permeability parameter, α – thermal diffusivity of the fluid, Q_0 – dimensional heat generation parameter, c_p – specific heat at constant pressure, and q_r – radiative flux vector respectively.

We should in prior warn the reader that our model is not the same as that by Jha and Aina, in which the magnetic parameter, permeability parameter, heat generation parameter, and radiation parameter were not taken into account. The corresponding boundary conditions of the micro-porous-channel fluid velocity and temperature can be written as

$$\left.\begin{aligned} u &= \frac{\lambda\left(2-F_v\right)}{F_v}\frac{du}{dy}, T = T_2 + \frac{2\gamma\lambda\left(2-F_t\right)}{Pr\,F_t\left(\gamma+1\right)}\frac{dT}{dy} \quad \text{at} \quad y=0 \\ u &= -\frac{\lambda\left(2-F_v\right)}{F_v}\frac{du}{dy}, T = T_1 - \frac{2\gamma\lambda\left(2-F_t\right)}{Pr\,F_t\left(\gamma+1\right)}\frac{dT}{dy} \quad \text{at} \quad y=a \end{aligned}\right\} \tag{4}$$

Here F_v – tangential momentum accommodation coefficient, F_t – tangential thermal accommodation coefficient, T_1 – hot wall temperature, T_2 – cold wall temperature, c_v – specific heat at constant volume, $\gamma = {c_p}/{c_v}$ – a ratio of specific heats, Pr – Prandtl number, λ – molecular mean free path, and a – distance between two plates respectively.

The radiative flux vector for an optically thick fluid can be written as (see, Venkateswarlu et al. & Hayat et al.)

$$q_r = -\frac{4\sigma^*}{3a*}\frac{dT^4}{dy} \tag{5}$$

Assuming a small difference between the fluid temperature T and the free stream temperature T_0 within the flow T^4 can be expressed in the Taylor series about T_0 and neglecting the second & higher-order terms in the series, we have

$$T^4 \cong 4T_0^3T - 3T_0^4 \tag{6}$$

Using equations (5) and (6) in equation (3), we obtain

$$\alpha\left[1+\frac{16\sigma^*T_0^3}{3a^*k_T}\right]\frac{d^2T}{dy^2} + \frac{Q_o}{\rho c_p}\left(T-T_0\right) + \frac{\nu}{c_p}\left[\frac{du}{dy}\right]^2 = 0 \tag{7}$$

The following non-dimensional variables are introduced

$$\left.\begin{aligned} &\eta = \frac{y}{a}, \theta = \frac{T-T_0}{T_1-T_0}, U = \frac{\nu u}{g\beta_T a^2\left(T_1-T_0\right)}, Pr = \frac{\nu}{\alpha}, \xi = \frac{T_2-T_0}{T_1-T_0}, \\ &\beta_v = \frac{2-F_v}{F_v}, \beta_t = \frac{2\gamma\left(2-F_t\right)}{Pr\,F_t\left(\gamma+1\right)}, kn = \frac{\lambda}{a}, ln = \frac{\beta_t}{\beta_v} \end{aligned}\right\} \tag{8}$$

Equations (2) and (7) reduce to the following non-dimensional form

$$\frac{d^2U}{d\eta^2}+\theta-\left[M+\frac{1}{K}\right]U=0 \tag{9}$$

$$\left[1+\frac{4}{3R}\right]\frac{d^2\theta}{d\eta^2}+Ec\left[\frac{dU}{d\eta}\right]^2+H\theta=0 \tag{10}$$

Here $M=\frac{\sigma B_0^2 a^2}{\rho\nu}$ is the magnetic parameter, $K=\frac{K_1}{a^2}$ is the permeability parameter, $R=\frac{a^* k_T}{4\sigma^* T_0^3}$ is the thermal radiation parameter, $H=\frac{Q_o a^2}{k_T}$ is the heat generation parameter and $Ec=\frac{\rho g^2 \beta_T^2 a^4 (T_1-T_0)}{\nu k_T}$ is the Eckert number respectively.

The corresponding boundary conditions in non-dimensional form can be written as

$$\left.\begin{aligned} U&=\beta_v kn\frac{dU}{d\eta},\ \theta=\xi+\beta_v kn\ln\frac{d\theta}{d\eta} \quad \text{at} \quad \eta=0\\ U&=-\beta_v kn\frac{dU}{d\eta},\ \theta=1-\beta_v kn\ln\frac{d\theta}{d\eta} \quad \text{at} \quad \eta=1\end{aligned}\right\} \tag{11}$$

It is now important to calculate the physical quantities of our primary interest, which are the local wall shear stress or skin friction coefficient and the local surface heat flux. Given the micro-porous–channel slip velocity and temperature fields in the boundary layer, the shear stress τ_w and the heat flux q_w are obtained as

$$\tau_w=\nu\left[\frac{du}{dy}\right] \tag{12}$$

$$q_w = -\alpha\left[\frac{dT}{dy}\right] \tag{13}$$

In the non-dimensional form, the skin-friction coefficient Cf and heat transfer coefficient Nu are defined as

$$Cf = \frac{\tau_w}{g\beta_T a(T_1 - T_0)} \tag{14}$$

$$Nu = \left[1 + \frac{4}{3R}\right]\frac{aq_w}{\alpha\left(T_1 - T_0\right)} \tag{15}$$

Using the non-dimensional variables in equation (11) and equations (12) to (13) into equations (14) to (15), we obtain the physical parameters

$$Cf = \left[\frac{dU}{d\eta}\right] \tag{16}$$

$$Nu = -\left[1 + \frac{4}{3R}\right]\left[\frac{d\theta}{d\eta}\right] \tag{17}$$

2. Solution of the Problem

Equations (9) and (10) are coupled non-linear ordinary differential equations and these cannot be solved in closed form. So, we reduce these non-linear ordinary differential equations into a set of ordinary differential equations, which can be solved analytically. This can be done by assuming the trial solutions, for the micro-porous–channel slip velocity and temperature of the fluid as (see, Jha and Aina, Venkateswarlu and Makinde)

$$U(\eta) = U_0(\eta) + EcU_1(\eta) + 0\left(Ec^2\right) \tag{18}$$

$$\theta(\eta) = \theta_o(\eta) + Ec\theta_1(\eta) + 0\left(Ec^2\right) \tag{19}$$

On substituting the equations (18) and (19) into the equations (9) and (10), then equating the harmonic and non-harmonic terms and neglecting the higher-order terms $0\left(Ec^2\right)$, we obtain

$$\frac{d^2U_0}{d\eta^2}+\theta_0-\left[M+\frac{1}{K}\right]U_0=0 \tag{20}$$

$$\frac{d^2U_1}{d\eta^2}+\theta_1-\left[M+\frac{1}{K}\right]U_1=0 \tag{21}$$

$$\left[1+\frac{4}{3R}\right]\frac{d^2\theta_0}{d\eta^2}+H\theta_0=0 \tag{22}$$

$$\left[1+\frac{4}{3R}\right]\frac{d^2\theta_1}{d\eta^2}+H\theta_1+\left[\frac{dU_0}{d\eta}\right]^2=0 \tag{23}$$

The corresponding boundary conditions can be written as

$$\left.\begin{aligned}
&U_0=\beta_v kn\frac{dU_0}{d\eta},U_1=\beta_v kn\frac{dU_1}{d\eta},\\
&\theta_0=\xi+\beta_v kn\ln\frac{d\theta_0}{d\eta},\theta_1=\beta_v kn\ln\frac{d\theta_1}{d\eta} \quad \text{at } \eta=0\\
&U_0=-\beta_v kn\frac{dU_0}{d\eta},U_1=-\beta_v kn\frac{dU_1}{d\eta},\\
&\theta_0=1-\beta_v kn\ln\frac{d\theta_0}{d\eta},\theta_1=-\beta_v kn\ln\frac{d\theta_1}{d\eta} \text{ at } \eta=1
\end{aligned}\right\} \tag{24}$$

The analytical solutions of the equations (20) to (23) with the boundary conditions in equation (24) are given by

$$U_0(\eta)=a_9\cos(m_1\eta)+a_{10}\sin(m_1\eta)+a_{20}\exp\left(-m_2\eta\right)+a_{21}\exp\left(m_2\eta\right) \tag{25}$$

$$\begin{aligned} U_1(\eta) = {} & a_{69} + b_1 \exp\left(-m_2\eta\right) + b_2 \exp\left(m_2\eta\right) - a_{68} \sin(2m_1\eta) + \\ & a_{67} \cos(2m_1\eta) + a_{66} \exp(m_2\eta) \sin(m_1\eta) + \\ & a_{65} \exp(m_2\eta) \cos(m_1\eta) + a_{64} \exp(-m_2\eta) \sin(m_1\eta) + \\ & a_{63} \exp(-m_2\eta) \cos(m_1\eta) + a_{61} \exp\left(2m_2\eta\right) + \\ & a_{60} \exp\left(-2m_2\eta\right) + a_{59} \sin(m_1\eta) + a_{58} \cos(m_1\eta) \end{aligned} \tag{26}$$

$$\theta_0(\eta) = a_6 \cos(m_1\eta) + a_7 \sin\left(m_1\eta\right) \tag{27}$$

$$\begin{aligned} \theta_1(\eta) = {} & a_{35} - a_{32} \sin(2m_1\eta) + a_{31} \cos(2m_1\eta) + \\ & a_{30} \exp(m_2\eta) \sin(m_1\eta) - a_{29} \exp(m_2\eta) \cos(m_1\eta) - \\ & a_{28} \exp(-m_2\eta) \sin(m_1\eta) + a_{27} \exp(-m_2\eta) \cos(m_1\eta) - \\ & a_{26} \exp\left(2m_2\eta\right) - a_{25} \exp\left(-2m_2\eta\right) + \\ & a_{57} \sin(m_1\eta) + a_{56} \cos(m_1\eta) \end{aligned} \tag{28}$$

On substituting the equations (25) to (28) into the equations (18) and (19), we obtained the expressions for the micro-porous–channel slip velocity and temperature as follows

$$\begin{aligned} U\left(\eta\right) = {} & \begin{bmatrix} a_9 \cos(m_1\eta) + a_{10} \sin(m_1\eta) + \\ a_{20} \exp\left(-m_2\eta\right) + a_{21} \exp\left(m_2\eta\right) \end{bmatrix} + \\ & Ec \begin{bmatrix} a_{69} + b_1 \exp\left(-m_2\eta\right) + b_2 \exp\left(m_2\eta\right) - a_{68} \sin(2m_1\eta) + \\ a_{67} \cos(2m_1\eta) + a_{66} \exp(m_2\eta) \sin(m_1\eta) + \\ a_{65} \exp(m_2\eta) \cos(m_1\eta) + a_{64} \exp(-m_2\eta) \sin(m_1\eta) + \\ a_{63} \exp(-m_2\eta) \cos(m_1\eta) + a_{61} \exp\left(2m_2\eta\right) + \\ a_{60} \exp\left(-2m_2\eta\right) + a_{59} \sin(m_1\eta) + a_{58} \cos(m_1\eta) \end{bmatrix} \end{aligned} \tag{29}$$

$$\begin{aligned} \theta\left(\eta\right) = {} & \left[a_6 \cos(m_1\eta) + a_7 \sin\left(m_1\eta\right) \right] + \\ & Ec \begin{bmatrix} a_{35} - a_{32} \sin(2m_1\eta) + a_{31} \cos(2m_1\eta) + \\ a_{30} \exp(m_2\eta) \sin(m_1\eta) - a_{29} \exp(m_2\eta) \cos(m_1\eta) - \\ a_{28} \exp(-m_2\eta) \sin(m_1\eta) + a_{27} \exp(-m_2\eta) \cos(m_1\eta) - \\ a_{26} \exp\left(2m_2\eta\right) - a_{25} \exp\left(-2m_2\eta\right) + \\ a_{57} \sin(m_1\eta) + a_{56} \cos(m_1\eta) \end{bmatrix} \end{aligned} \tag{30}$$

3.1. Skin friction: From the micro-porous–channel slip velocity, the skin friction coefficient at the plates can be expressed as

$$Cf = \left[m_1 a_{10} \cos(m_1\eta) - m_1 a_9 \sin(m_1\eta) - m_2 a_{20} \exp(-m_2\eta) + m_2 a_{21} \exp(m_2\eta) \right] + Ec \begin{bmatrix} m_2 b_2 \exp(m_2\eta) + a_{71} \cos(m_1\eta) + a_{73} \exp(2m_2\eta) + \\ a_{75} \exp(-m_2\eta)\cos(m_1\eta) + a_{77} \exp(m_2\eta)\cos(m_1\eta) - \\ m_2 b_1 \exp(-m_2\eta) - a_{70} \sin(m_1\eta) - a_{72} \exp(-2m_2\eta) - \\ a_{74} \exp(-m_2\eta)\sin(m_1\eta) - a_{76} \exp(m_2\eta)\sin(m_1\eta) - \\ a_{78} \sin(2m_1\eta) - a_{79} \cos(2m_1\eta) \end{bmatrix} \quad (31)$$

3.2. Nusselt number: From the temperature of the fluid, the heat transfer coefficient at the plates can be expressed as

$$Nu = -\left[1 + \frac{4}{3R}\right]\left[m_1 a_8 \cos(m_1\eta) - m_1 a_7 \sin(m_1\eta) \right] - Ec\left[1 + \frac{4}{3R}\right] \begin{bmatrix} m_1 a_{57} \cos(m_1\eta) + a_{36} \exp(-2m_2\eta) + \\ a_{40} \exp(m_2\eta)\sin(m_1\eta) + a_{41} \exp(m_2\eta)\cos(m_1\eta) - \\ m_1 a_{56} \sin(m_1\eta) - a_{37} \exp(2m_2\eta) - \\ a_{38} \exp(-m_2\eta)\sin(m_1\eta) - \\ a_{39} \exp(-m_2\eta)\cos(m_1\eta) - \\ a_{42} \sin(2m_1\eta) - a_{43} \cos(2m_1\eta) \end{bmatrix} \quad (32)$$

4. Results and Discussion

To discuss the influence of various flow parameters like a magnetic parameter M, permeability parameter K, radiation parameter R, heat generation parameter H, Eckert number Ec, Knudsen number kn, and fluid wall interaction parameter ln in the presence of wall ambient temperature difference ratio ξ on the convective heat transfer, the numerical results of the micro-channel slip velocity U, temperature θ, skin friction coefficient Cf, and heat transfer coefficient Nu are computed. This discussion has been performed over the reasonable ranges of $0 \le \beta_v kn \le 0.1$ and $0 \le ln \le 10$. The selected reference values for the present discussion are $\beta_v = 1$, $kn = 0.05$, $ln = 1.667$, $M = 1$, $K = 1$, $R = 1$, $H = 1$, and $Ec = 0.01$ respectively. This study $\xi = -0.5$ corresponds to one wall is heating

and one wall is cooling, $\xi = 0.0$ corresponds to one wall is heating and one wall is not heating and $\xi = 0.5$ corresponds to both walls are heated.

Fig. 2 displays the combined influence of the magnetic parameter M and wall ambient temperature difference ratio ξ on the micro-channel slip velocity U. It is seen that increasing the values of the magnetic parameter tends to slow down the slip velocity of the fluid in the micro-channel. The impact of magnetic parameter on the micro-channel slip velocity becomes significant with an increase in the wall-ambient temperature difference ratio. Fig. 3 shows the impact of the permeability parameter K as well as wall-ambient temperature difference ratio ξ on the micro-channel slip velocity U. Increasing the value of the permeability parameter leads to enhancement in the micro-channel slip velocity. The permeability parameter is found to be an increasing function of the wall-ambient temperature difference ratio.

Figs. 4 and 5 illustrate the influence of radiation parameter R, heat generation parameter H and wall ambient temperature difference ratio ξ on the micro-channel slip velocity U. It is noticed that the micro-channel slip velocity increases with an increase in the radiation parameter or heat generation parameter. This fact is justified because the fluid temperature θ increases with an increase in the radiation parameter or heat generation parameter as observed from Figs. 9 and 10. This implies that the fluid temperature strengthens the thermal buoyancy force. Therefore micro–channel slip velocity is getting accelerated with an increase in the radiation parameter or heat generation parameter. However, it is worth noting that the influence of radiation parameter and heat generation parameter becomes significantly pronounced in the presence of symmetric heating.

Fig. 6 displays the influence of Eckert number Ec as well as wall ambient temperature difference ratio ξ on the micro-channel slip velocity U. It is noticed that the micro-channel slip velocity attain their steady state with an increase in the Eckert number and the micro-channel slip velocity increases on increasing the wall ambient temperature difference ratio. Fig. 7 shows the combined influence of Knudsen number kn and wall ambient temperature

difference ratio ξ on the micro-channel slip velocity U. It is observed that the micro-channel slip velocity increases with an increase in the Knudsen number. The effect of the Knudsen number is more pronounced in presence of symmetric heating.

Fig. 8 demonstrates the effect of fluid wall interaction parameters ln on the micro-channel slip velocity U in three different cases of wall ambient temperature difference ratio ξ. It is noticed that there is an enhancement in the micro-channel slip velocity at the cold wall and a reduction in the micro-channel slip velocity at the heated wall with an increase in the fluid wall interaction parameter in the presence of $\xi = -0.5$ whereas there is an enhancement in the micro-channel slip velocity on increasing the fluid wall interaction parameter in the presence of $\xi = 0.0$ and $\xi = 0.5$.

Fig. 9 and 10 reveals the influence of radiation parameter R and heat generation parameter H on the fluid temperature θ in the presence of wall ambient temperature difference ratio ξ. It is noticed that the fluid temperature increases with an increase in the radiation parameter or heat generation parameter. Furthermore, the influence of the radiation parameter and heat generation parameter on the fluid temperature becomes significant in the case of symmetric heating.

Fig. 11 exhibits the combined impact of Eckert number Ec and wall ambient temperature difference ratio ξ on the fluid temperature θ. It is found that the fluid temperature attains its steady state with an increase in the Eckert number and hence there is an enhancement in the fluid temperature with an increase in the wall ambient temperature difference ratio.

Fig. 12 and 13 exhibits the influence of Knudsen number kn and fluid wall interaction parameter ln on the fluid temperature θ respectively in three distinct cases of wall ambient temperature difference ratio ξ. It is noticed that there is an enhancement at the cold wall and a reduction at the hot wall in the fluid temperature with an increase in the Knudsen number or fluid wall interaction parameter.

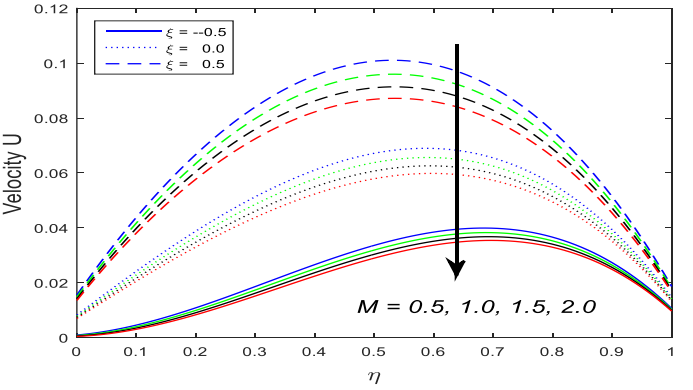

Fig.2: Impact of magnetic parameter on the micro-channel velocity

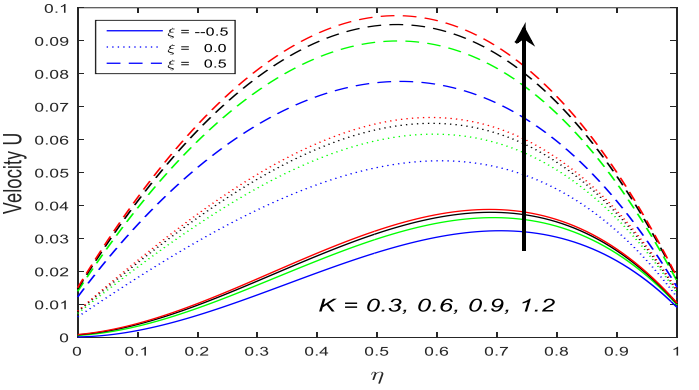

Fig. 3: Impact of permeability parameter on the micro-channel velocity

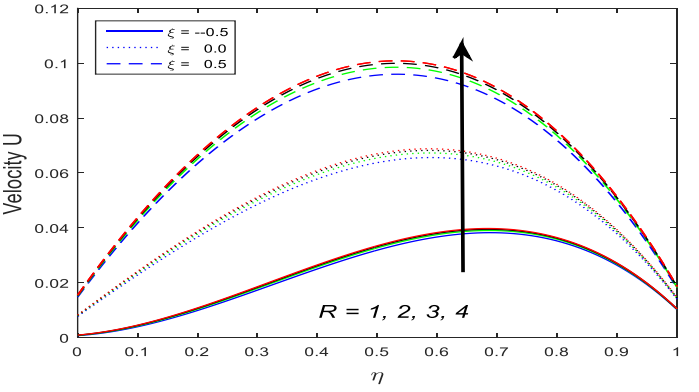

Fig. 4: Impact of radiation parameter on the micro-channel velocity

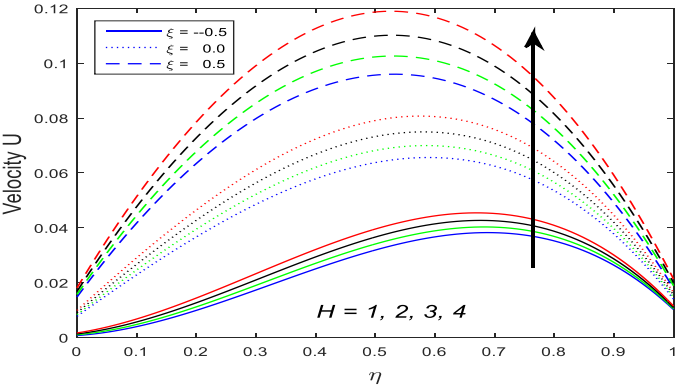

Fig. 5: Impact of heat generation parametet on the micro-channel velocity

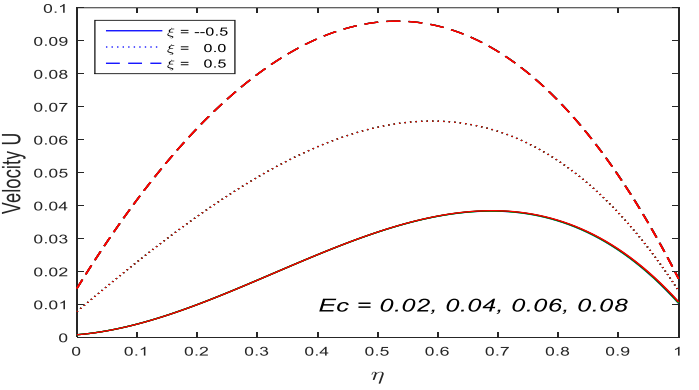

Fig.6: Impact of Eckert number on the micro-channel velocity

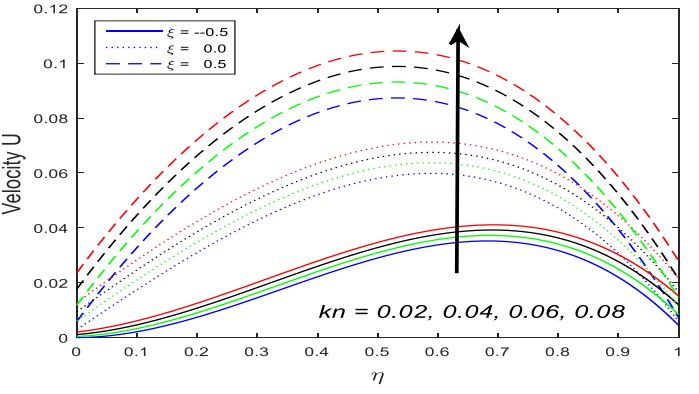

Fig. 7: Impact of Knudsen number on the micro-channel slip velocity

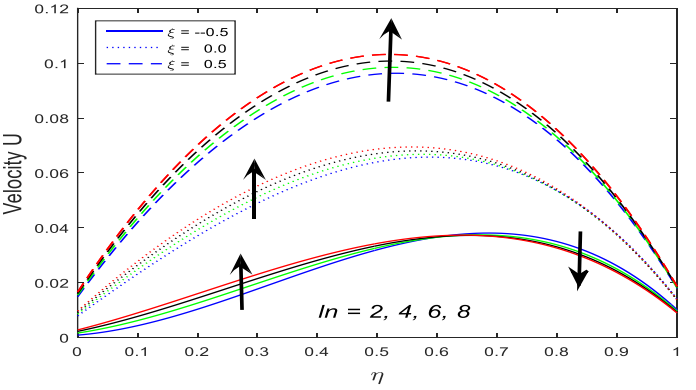

Fig. 8: Impact of fluid wall interaction parameter on the micro-channel velocity

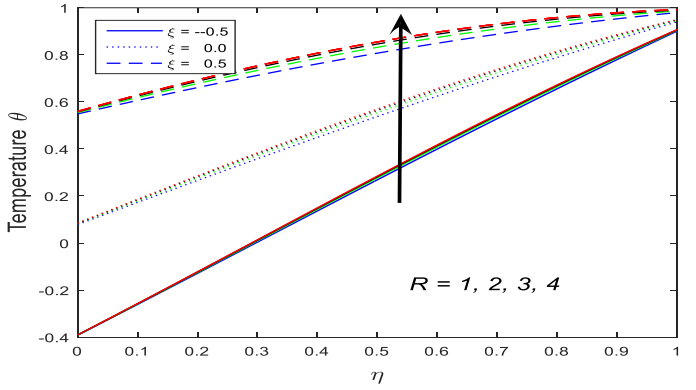

Fig. 9: Impact of radiation parameter on the fluid temperature

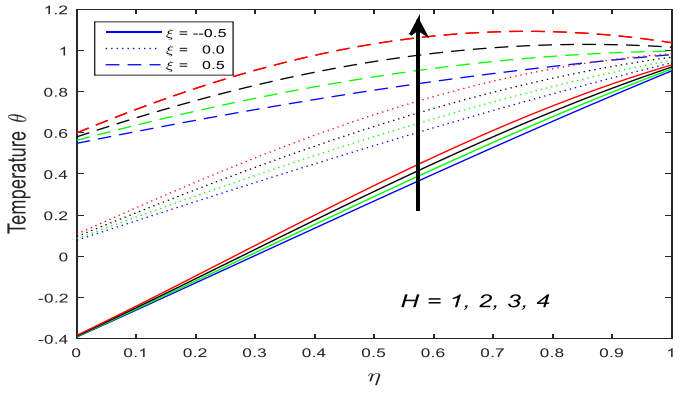

Fig. 10: Impact of heat generation parameter on the fluid temperature

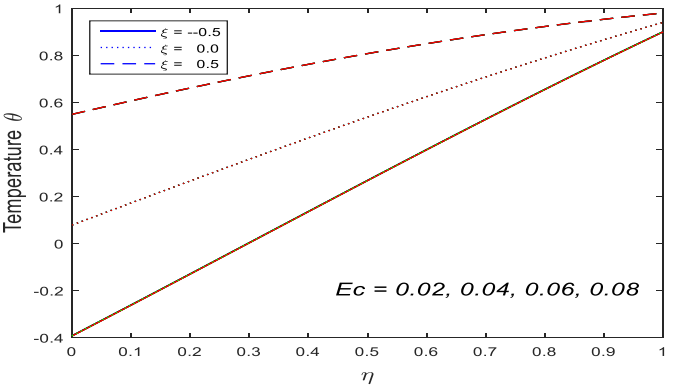

Fig. 11: Impact of Eckert number on the fluid temperature

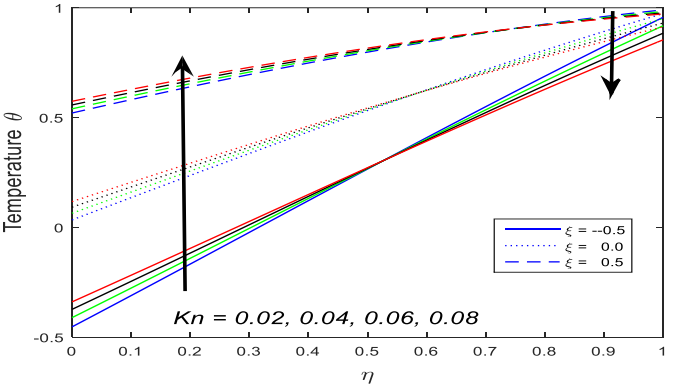

Fig. 12: Impact of Knudsen number on the fluid temperature

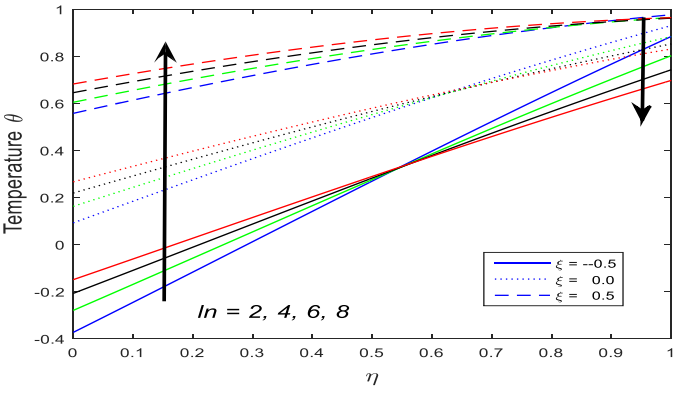

Fig. 13: Impact of fluid wall interaction parameter on the fluid temperature

The skin friction coefficient Cf at the cold wall ($\eta = 0$) and the hot wall ($\eta = 1$) for various values of the magnetic parameter M, permeability parameter K, radiation parameter R, heat generation parameter H, Eckert number Ec, Knudsen number kn, and fluid wall interaction parameter ln are presented in tables 1 to 7 in three cases of wall ambient temperature difference ratio ξ. It is found that the skin friction coefficient decreases at the cold wall and increases at the hot wall with an increase in the magnetic parameter in the case of asymmetric heating and symmetric heating. It is noticed that there is an enhancement at the cold wall and a reduction at the hot wall in the skin friction coefficient with an increase in the permeability parameter, radiation parameter or heat generation parameter in the case of asymmetric heating and symmetric heating. It is noticed that the skin friction coefficient decreases at the cold wall and increases at the hot wall with an increase in the Eckert number in case of asymmetric heating whereas Cf attains their steady-state at the cold wall and decreases at the hot wall in case of symmetric heating. Skin friction coefficient increases at both cold and hot walls with an increase in the Knudsen number in the case of asymmetric heating and symmetric heating. There is an enhancement at the cold wall and a reduction at the hot wall in the skin friction coefficient with an increase in the fluid wall interaction parameter in case of symmetric heating whereas the fluid wall interaction parameter enhanced the skin friction coefficient at both cold and hot walls in case of asymmetric heating.

The rate of heat transfer Nu at the cold wall ($\eta = 0$) and the hot wall ($\eta = 1$) for various values of radiation parameter R, heat generation parameter H, Eckert number Ec, Knudsen number kn, and fluid wall interaction parameter ln are presented in tables 8 to 12 in three cases of wall ambient temperature difference ratio ξ. It is clear that, the heat transfer coefficient increases at both cold and hot walls with an increase in the radiation parameter, Knudsen number and fluid wall interaction parameter in case of asymmetric heating and symmetric heating. It is noticed that there is a reduction at the cold wall and an enhancement at the hot wall in the heat transfer coefficient with an increase in the heat generation parameter in the case of asymmetric heating and symmetric heating. Heat transfer

coefficient decreases at both cold and hot walls on increasing the Eckert number $\xi = -0.5$. There is a reduction at the cold wall and an enhancement at the hot wall in the heat transfer coefficient with an increase in the Eckert number for $\xi = 0.0$ and $\xi = 0.5$.

Table 1: Impact of magnetic parameter on the skin friction coefficient

M	$\xi = -0.5$		$\xi = 0.0$		$\xi = 0.5$	
	Cold wall	Hot wall	Cold wall	Hot wall	Cold wall	Hot wall
0.5	0.0186	-0.2087	0.1642	-0.2911	0.3098	-0.3733
1.0	0.0148	-0.2028	0.1551	-0.2806	0.2954	-0.3582
1.5	0.0114	-0.1974	0.1469	-0.2710	0.2824	-0.3445
2.0	0.0084	-0.1923	0.1395	-0.2622	0.2706	-0.3320

Table 2: Impact of permeability parameter on the skin friction coefficient

K	$\xi = -0.5$		$\xi = 0.0$		$\xi = 0.5$	
	Cold wall	Hot wall	Cold wall	Hot wall	Cold wall	Hot wall
0.3	0.0018	-0.1805	0.1227	-0.2419	0.2437	-0.3033
0.6	0.0104	-0.1957	0.1444	-0.2679	0.2784	-0.3402
0.9	0.0140	-0.2016	0.1532	-0.2783	0.2924	-0.3551
1.2	0.0160	-0.2047	0.1581	-0.2839	0.3001	-0.3631

Table 3: Impact of radiation parameter on the skin friction coefficient

R	$\xi = -0.5$		$\xi = 0.0$		$\xi = 0.5$	
	Cold wall	Hot wall	Cold wall	Hot wall	Cold wall	Hot wall
1.0	0.0148	-0.2028	0.1551	-0.2806	0.2954	-0.3582
2.0	0.0168	-0.2059	0.1598	-0.2859	0.3028	-0.3659
3.0	0.0180	-0.2075	0.1625	-0.2889	0.3069	-0.3702
4.0	0.0187	-0.2086	0.1641	-0.2908	0.3095	-0.3729

Table 4: Impact of heat generation parameter on the skin friction coefficient

H	$\xi = -0.5$		$\xi = 0.0$		$\xi = 0.5$	
	Cold wall	Hot wall	Cold wall	Hot wall	Cold wall	Hot wall
1.0	0.0148	-0.2028	0.1551	-0.2806	0.2954	-0.3582
2.0	0.0202	-0.2107	0.1674	-0.2944	0.3146	-0.3781
3.0	0.0264	-0.2193	0.1814	-0.3101	0.3364	-0.4008
4.0	0.0337	-0.2291	0.1977	-0.3280	0.3617	-0.4269

Table 5: Impact of Eckert number on the skin friction coefficient

Ec	$\xi = -0.5$		$\xi = 0.0$		$\xi = 0.5$	
	Cold wall	Hot wall	Cold wall	Hot wall	Cold wall	Hot wall
0.02	0.0148	-0.2026	0.1551	-0.2805	0.2955	-0.3583
0.04	0.0147	-0.2022	0.1551	-0.2804	0.2955	-0.3584
0.06	0.0146	-0.2018	0.1550	-0.2804	0.2955	-0.3585
0.08	0.0146	-0.2014	0.1550	-0.2803	0.2955	-0.3586

Table 6: Impact of Knudsen number on the skin friction coefficient

kn	$\xi = -0.5$		$\xi = 0.0$		$\xi = 0.5$	
	Cold wall	Hot wall	Cold wall	Hot wall	Cold wall	Hot wall
0.02	0.0010	-0.2197	0.1479	-0.2938	0.2949	-0.3679
0.04	0.0106	-0.2080	0.1530	-0.2847	0.2953	-0.3613
0.06	0.0187	-0.1979	0.1571	-0.2767	0.2955	-0.3553
0.08	0.0257	-0.1891	0.1605	-0.2695	0.2958	-0.3499

Table 7: Impact of fluid wall interaction parameter on the skin friction coefficient

ln	$\xi = -0.5$		$\xi = 0.0$		$\xi = 0.5$	
	Cold wall	Hot wall	Cold wall	Hot wall	Cold wall	Hot wall
2.0	0.0178	-0.2007	0.1576	-0.2797	0.2975	-0.3586
4.0	0.0330	-0.1905	0.1712	-0.2763	0.3094	-0.3620
6.0	0.0453	-0.1836	0.1830	-0.2752	0.3207	-0.3668
8.0	0.0556	-0.1789	0.1936	-0.2750	0.3316	-0.3727

Table 8: Impact of radiation parameter on the heat transfer coefficient

R	$\xi = -0.5$		$\xi = 0.0$		$\xi = 0.5$	
	Cold wall	Hot wall	Cold wall	Hot wall	Cold wall	Hot wall
1.0	-3.0391	-2.7750	-2.2023	-1.6737	-1.3655	-0.5724
2.0	-2.1846	-1.9143	-1.6367	-1.0958	-1.0889	-0.2773
3.0	-1.9004	-1.6266	-1.4496	-0.9017	-0.9988	-0.1767
4.0	-1.7585	-1.4824	-1.3564	-0.8041	-0.9545	-0.1257

Table 9: Impact of heat generation parameter on the heat transfer coefficient

H	$\xi = -0.5$		$\xi = 0.0$		$\xi = 0.5$	
	Cold wall	Hot wall	Cold wall	Hot wall	Cold wall	Hot wall
1.0	-3.0391	-2.7750	-2.2023	-1.6737	-1.3655	-0.5724
2.0	-3.0920	-2.5314	-2.4352	-1.3137	-1.7784	-0.0960
3.0	-3.1620	-2.2658	-2.7055	-0.9130	-2.2491	0.4399
4.0	-3.2534	-1.9737	-3.0222	-0.4625	-2.7910	1.0487

Table 10: Impact of Eckert number on the heat transfer coefficient

Ec	$\xi = -0.5$		$\xi = 0.0$		$\xi = 0.5$	
	Cold wall	Hot wall	Cold wall	Hot wall	Cold wall	Hot wall
0.02	-3.0391	-2.7752	-2.2023	-1.6737	-1.3657	-0.5722
0.04	-3.0391	-2.7755	-2.2025	-1.6736	-1.3660	-0.5718
0.06	-3.0392	-2.7758	-2.2026	-1.6735	-1.3663	-0.5713
0.08	-3.0392	-2.7761	-2.2027	-1.6735	-1.3667	-0.5709

Table 11: Impact of Knudsen number on the heat transfer coefficient

kn	$\xi = -0.5$		$\xi = 0.0$		$\xi = 0.5$	
	Cold wall	Hot wall	Cold wall	Hot wall	Cold wall	Hot wall
0.02	-3.3010	-3.0397	-2.3749	-1.8522	-1.4489	-0.6646
0.04	-3.1214	-2.8583	-2.2565	-1.7299	-1.3916	-0.6015
0.06	-2.9613	-2.6962	-2.1510	-1.6205	-1.3409	-0.5448
0.08	-2.8176	-2.5506	-2.0566	-1.5221	-1.2957	-0.4935

Table 12: Impact of fluid wall interaction parameter on the heat transfer coefficient

ln	$\xi = -0.5$		$\xi = 0.0$		$\xi = 0.5$	
	Cold wall	Hot wall	Cold wall	Hot wall	Cold wall	Hot wall
2.0	-2.9613	-2.6963	-2.1511	-1.6206	-1.3409	-0.5448
4.0	-2.5708	-2.2996	-1.8949	-1.3520	-1.2190	-0.4043
6.0	-2.2766	-1.9990	-1.7030	-1.1472	-1.1295	-0.2954
8.0	-2.0473	-1.7629	-1.5547	-0.9853	-1.0622	-0.2076

5. Conclusion

This study considered the influence of heat generation and thermal radiation on steady hydromagnetic fully developed natural convection flow of an incompressible and electrically conducting fluid in a vertical micro-porous–channel in presence of viscous dissipation. The main observations of the presented research are listed below:

- It is found that the micro-channel slip velocity and fluid temperature are increasing functions of radiation parameter and heat generation parameter while micro–channel slip velocity is a decreasing function of the magnetic parameter.
- It is observed that the micro-channel slip velocity and fluid temperature are constant functions of Eckert number while micro–channel slip velocity is an increasing function of permeability parameter.
- Skin friction coefficient increases at the cold wall and decreases at the hot wall with an increase in permeability parameter, radiation parameter and heat generation parameter while the reverse trend is observed in the case of the magnetic parameter.
- The rate of heat transfer increases with the increase of radiation parameter at both cold and hot walls whereas

there is a reduction at the cold wall and an enhancement at the hot wall in the case of heat generation parameter.

Acknowledgements

The authors wish to appreciate the constructive suggestions and comments of the anonymous reviewers.

Appendix

$$m_1 = \sqrt{\frac{H}{a_1}}, m_2 = \sqrt{M + \frac{1}{K}}, a_1 = 1 + \frac{4}{3R}, a_2 = \beta_v \, kn \ln m_1,$$

$$a_3 = a_2 \sin(m_1), a_4 = a_2 \cos(m_1), a_5 = \cos(m_1) - a_3, a_6 = \sin(m_1) + a_4,$$

$$a_7 = \frac{a_2 + a_6\xi}{a_2 a_5 + a_6}, a_8 = \frac{1 - a_5\xi}{a_2 a_5 + a_6}, a_9 = \frac{a_7}{m_1^2 + m_2^2}, a_{10} = \frac{a_8}{m_1^2 + m_2^2},$$

$$a_{11} = \beta_v \, kn \, m_2, a_{12} = 1 + a_{11}, a_{13} = 1 - a_{11}, a_{14} = \beta_v \, kn \, m_1 \, a_{10} - a_9,$$

$$a_{15} = a_{13} \exp(-m_2), a_{16} = a_{12} \exp(m_2), a_{17} = \beta_v \, kn \, m_1 \, a_9 - a_{10},$$

$$a_{18} = \beta_v \, kn \, m_1 \, a_{10} + a_9, a_{19} = a_{17} \sin(m_1) - a_{18} \cos(m_1),$$

$$a_{20} = \frac{a_{14}a_{16} - a_{13}a_{19}}{a_{12}a_{16} - a_{13}a_{15}}, a_{21} = \frac{a_{14}a_{15} - a_{12}a_{19}}{a_{13}a_{15} - a_{12}a_{16}}, a_{22} = \frac{m_2^2}{a_1\left(4m_2^2 + m_1^2\right)},$$

$$a_{23} = \frac{2m_1m_2}{a_1\left(4m_1^2 + m_2^2\right)}, \; a_{24} = \frac{4m_1^2}{a_1\left(4m_1^2 + m_2^2\right)}, \; a_{25} = a_{22}a_{20}^2, \; a_{26} = a_{22}a_{21}^2,$$

$$a_{27} = a_{20}(a_{10}a_{23} - a_9a_{24}), a_{28} = a_{20}(a_9a_{23} + a_{10}a_{24}),$$

$$a_{29} = a_{21}(a_{10}a_{23} + a_9a_{24}), a_{30} = a_{21}(a_9a_{23} - a_{10}a_{24}), a_{31} = \frac{a_{10}^2 - a_9^2}{6a_1},$$

$$a_{32} = \frac{a_9a_{10}}{3a_1}, a_{33} = \frac{2m_2^2a_{20}a_{21}}{m_1^2a_1}, a_{34} = \frac{a_9^2 + a_{10}^2}{2a_1}, a_{35} = a_{33} - a_{34},$$

$a_{36} = 2m_2 a_{25}$, $a_{37} = 2m_2 a_{26}$, $a_{38} = m_1 a_{27} - m_2 a_{28}$, $a_{39} = m_1 a_{28} + m_2 a_{27}$,

$a_{40} = m_1 a_{29} + m_2 a_{30}$, $a_{41} = m_1 a_{30} - 70 m_2 a_{29}$, $a_{42} = 2m_1 a_{31}$, $a_{43} = 2m_1 a_{32}$,

$a_{44} = (a_{27} + a_{31} + a_{35}) - (a_{25} + a_{26} + a_{29})$,

$a_{45} = (a_{36} + a_{41}) - (a_{37} + a_{39} + a_{43})$, $a_{46} = \beta_v \; kn \ln a_{45} - a_{44}$,

$a_{47} = a_{27} \cos(m_1) \exp(-m_2) + a_{30} \sin(m_1) \exp(m_2) + a_{31} \cos(2m_1) + a_{35}$,

$a_{48} = a_{28} \sin(m_1) \exp(-m_2) + a_{29} \cos(m_1) \exp(m_2) +$

$a_{32} \sin(2m_1) + a_{25} \exp(-2m_2) + a_{26} \exp(2m_2)$.

$a_{49} = a_{36} \exp(-2m_2) + a_{40} \sin(m_1) \exp(m_2) + a_{41} \cos(m_1) \exp(m_2)$,

$a_{50} = a_{37} \exp(2m_2) + a_{38} \sin(m_1) \exp(-m_2) + a_{39} \cos(m_1) \exp(-m_2)$,

$a_{51} = a_{42} \sin(2m_1) + a_{43} \cos(2m_1)$, $a_{52} = a_{49} - (a_{50} + a_{51})$,

$a_{53} = \cos(m_1) - a_3$, $a_{54} = \sin(m_1) + a_4$, $a_{55} = a_{48} - (a_{47} + \beta_v \; kn \ln a_{52})$,

$a_{56} = \dfrac{a_{54} a_{46} - a_{55} a_2}{a_{54} + a_{53} a_2}$, $a_{57} = \dfrac{a_{55} - a_{53} a_{46}}{a_{54} + a_{53} a_2}$, $a_{58} = \dfrac{a_{56}}{m_1^2 + m_2^2}$, $a_{59} = \dfrac{a_{57}}{m_1^2 + m_2^2}$,

$a_{60} = \dfrac{a_{25}}{3m_2^2}$, $a_{61} = \dfrac{a_{26}}{3m_2^2}$, $a_{62} = \dfrac{1}{m_1\left(4m_2^2 + m_1^2\right)}$ $a_{63} = a_{62}(2m_2 a_{28} + m_1 a_{27})$

, $a_{64} = a_{62}(2m_2 a_{27} - m_1 a_{28})$, $a_{65} = a_{62}(2m_2 a_{30} - m_1 a_{29})$ m,

$a_{66} = a_{62}(2m_2 a_{29} + m_1 a_{30})$, $a_{67} = \dfrac{a_{31}}{4m_1^2 + m_2^2}$, $a_{68} = \dfrac{a_{32}}{4m_1^2 + m_2^2}$, $a_{69} = \dfrac{a_{35}}{m_2^2}$

, $a_{70} = m_1 a_{58}$, $a_{71} = m_1 a_{59}$, $a_{72} = 2m_2 a_{60}$, $a_{73} = 2m_2 a_{61}$

$a_{74} = a_{63} m_1 + a_{64} m_2$, $a_{75} = a_{64} m_1 - a_{63} m_2$, $a_{76} = a_{65} m_1 - a_{66} m_2$,

$a_{77} = a_{66} m_1 + a_{65} m_2$, $a_{78} = 2m_1 a_{67}$, $a_{79} = 2m_1 a_{68}$, $a_{80} = a_{58} + a_{60} + a_{61}$,

$a_{81} = a_{63} + a_{65} + a_{67} + a_{69}$, $a_{82} = a_{80} + a_{81}$, $a_{83} = a_{71} + a_{73} + a_{75} + a_{77}$,

$a_{84} = a_{79} + a_{72}$, $a_{85} = a_{83} - a_{84}$, $a_{86} = \beta_v \; kn \, a_{85} - a_{82}$,

$a_{87} = a_{59}\sin(m_1) + a_{58}\cos(m_1)$, $a_{88} = a_{60}\exp(-2m_2) + a_{61}\exp(2m_2)$,

$a_{89} = a_{63}\cos(m_1)\exp(-m_2) + a_{64}\sin(m_1)\exp(-m_2)$,

$a_{90} = a_{65}\cos(m_1)\exp(m_2) + a_{66}\sin(m_1)\exp(m_2)$,

$a_{91} = a_{67}\cos(2m_1) - a_{68}\sin(2m_1)$, $a_{92} = a_{69} + a_{87} + a_{88} + a_{89} + a_{90} + a_{91}$,

$a_{93} = a_{71}\cos(m_1) - a_{70}\sin(m_1)$, $a_{94} = a_{73}\exp(2m_2) - a_{72}\exp(-2m_2)$,

$a_{95} = a_{75}\cos(m_1)\exp(-m_2) - a_{74}\sin(m_1)\exp(-m_2)$,

$a_{96} = a_{77}\cos(m_1)\exp(m_2) - a_{76}\sin(m_1)\exp(m_2)$,

$a_{97} = a_{79}\cos(2m_1) + a_{78}\sin(2m_1)$, $a_{98} = (a_{93} + a_{94} + a_{95} + a_{96}) - a_{97}$,

$a_{99} = a_{92} + \beta_v \; kn\, a_{98}$, $b_1 = \dfrac{a_{86}a_{16} + a_{13}a_{99}}{a_{12}a_{16} - a_{13}a_{15}}$, $b_2 = \dfrac{a_{86}a_{15} + a_{12}a_{99}}{a_{13}a_{15} - a_{12}a_{16}}$.

References

K. Ali, S. Ahmad and M. Ashraf: Numerical simulation of flow and heat transfer in the hydromagnetic micropolar fluid between two stretchable disks with viscous dissipation effects, Journal of Theoretical and Applied Mechanics, Vol. 54, No. 2, 2016, 633–643.

A N. Altunkaya, M. Avci and O. Aydin: Effects of viscous dissipation on mixed convection In a vertical parallel plate microchannel with asymmetric uniform wall heat fluxes: The slip regime, International Journal of Heat and Mass Transfer, Vol. 111, 2017, 495–499.

M. Gnaneswara Reddy, P. Padma and B. Shankar: Effects of viscous dissipation and heat source on unsteady MHD flow over a stretching sheet, Ain Shams Engineering Journal, Vol. 6, No. 4, 2015, 1195–1201.

S. P. Anjali Devi and B. Ganga: Effects of viscous and joules dissipation on MHD flow, heat and mass transfer past a stretching porous surface embedded in a porous medium,

Nonlinear Analysis: Modelling and Control, Vol. 14, 2009, 303–314.

B. K. Jha and B. Aina: Impact of viscous dissipation on fully developed natural convection flow in a vertical micro-channel, Journal of Heat Transfer, Vol. 140, 2018, 094502, 1–7.

M. Venkateswarlu, G. V. Ramana Reddy and D. V. Lakshmi: Effects of chemical reaction and heat generation on MHD boundary layer flow of a moving vertical plate with suction and dissipation, Engineering International, Vol. 1, No. 1, 2013, 27–38.

A. Barletta: Laminar mixed convection with viscous dissipation in a vertical channel, Int. J. Heat Mass Transfer, Vol. 41, 1998, 3501–3513.

K. V. Prasad, P. Mallikarjun and H. Vaidya: Mixed convective fully developed flow in a vertical channel in the presence of thermal radiation and viscous dissipation, Int. J. of Applied Mechanics and Engineering, Vol. 22, No. 1, 2017, 123–144.

J. C. Umavathi and A. J. Chamkha: Combined effect of variable viscosity and thermal conductivity on free convection flow of a viscous fluid in a vertical channel, Int. J. Numer. Methods Heat Fluid Flow, Vol. 26, No. 1, 2016, 18–39.

B. K. Jha, B. Aina and A. T. Ajiya: MHD natural convection flow in a vertical parallel plate micro-channel, Ain Shams Engineering Journal, Vol. 5, 2014, 289–295.

B. Buonomo and O. Manca: Natural convection flow in a vertical micro-channel heated at uniform heat flux, Int. J. Therm. Sci, Vol. 49, 2012, 1333–1344.

O. Aydin and M. Avci: Thermally developing flow in micro-channels, J. Thermophys. Heat Transfer, Vol. 20, 2006, 628–632.

C. K. Chen and H. C. Weng: Natural convection in a vertical microchannel, J. Heat Transfer Trans, ASME, Vol. 127, 2005, 1053–1056.

O. M. Haddad, M. M. Abuzaid and M. A. Al-Nimr: Developing free-convection gas flow in a vertical open-ended micro-channel filled with porous media, Numer. Heat Transfer, Part A, Vol. 48, 2005, 693–710.

M. Venkateswarlu, O. D. Makinde and D. V. Lakshmi: Influence of thermal radiation and heat generation on steady hydromagnetic flow in a vertical micro-porous–channel in presence of suction/injection, Journal of Nanofluids, Vol. 8, No. 5, 1010–1019, 2019.

B. K. Jha and B. Aina: Mixed convection flow in a vertical micro–annulus having temperature-dependent viscosity: An exact solution, J. Nanofluids, Vol. 7, 2018, 1–8.

A. F. Khadrawi, A. Othman and M. A. Al – Nimr: Transient free convection fluid flow in a vertical micro-channel as described by the hyperbolic heat conduction model, Int. J. Thermophys, Vol. 26, 2005, 905–918.

H. Y. Wu and P. Cheng: An experimental study of convective heat transfer in silicon micro-channel with different surface conditions, International Journal of Heat and Mass Transfer, Vol. 46, 2003, 2547–2556.

B. K. Jha, B. Aina and S. B. Joseph: Natural convection flow in a vertical micro-channel with suction/injection, Journal of Process Mechanical Engineering, Vol. 228, 2014, 171–180.

K. R. Cramer and S. I. Pai: Magneto fluid dynamics for engineers and applied physicists, Mc Graw Hill Book Company, New York, 1973.

E. M. Sparrow and R. D. Cess: Temperature-dependent heat sources or sinks in a stagnation point flow, Appl. Sci. Res, Vol. 10, No. 1, 1961, 185–197.

T. Hayat, S. A. Shehzad and M. Qasim: Mixed convection flow of a micropolar fluid with radiation and chemical reaction, International Journal for Numerical Methods in Fluids, Vol. 67, No, 11, 2010, pp. 1418–1436.

M. Venkateswarlu and O. D. Makinde: Unsteady MHD slip flows with radiative heat and mass transfer over an inclined plate

embedded in a porous medium, Defect and Diffusion Forum, 384, 2018, 31–48.

H. R. Kataria and H. R. Patel: Radiation and chemical reaction effects on MHD Casson fluid flow past an oscillating vertical plate embedded in a porous medium, Alexandria Engineering Journal, Vol. 55 No. 1, 2016, 583–595.

V. Malapati and V. L. Dasari: Soret and chemical reaction effects on the radiative MHD flow from an infinite vertical plate, J. Korean Soc. Ind. Appl. Math., Vol. 21, No.1, 2017, 39–61.

G. S. Seth, S. M. Hussain and S. Sarkar: Hydromagnetic natural convection flow with heat and mass transfer of a chemically reacting and heat-absorbing fluid past and accelerated moving vertical plate with ramped temperature and ramped surface concentration through a porous medium, Journal of the Egyptian Mathematical Society, Vol. 23 No. 1, 2014, 197–207.

S. D. Adhikary and J. C. Misra: Unsteady two-dimensional hydromagnetic flow and heat transfer and heat transfer of a fluid, Int. J. of Appl. Math. & Mech, Vol. 7, No. 4, 2011, 1–20.

B. P. Garg, K. D. Singh and A. K. Bansal: Oscillatory MHD convective flow of second-order fluid through a porous medium in a vertical rotating channel in slip-flow regime with heat radiation, Int. J. of Applied Mechanics and Engineering, Vol. 20, 2015, 33–52.

B. K. Jha and B. Aina: Mathematical modelling and exact solution of steady fully developed mixed convection flow in a vertical micro–porous–annulus, J. Afrika Matematika, Vol. 26, 2015, 1199–1213.

M. Venkateswarlu, R. Vasu Babu and S. K. Mohiddin Shaw: Dufour and heat source effects on radiative MHD slip flow of a viscous fluid in a parallel porous plate channel in presence of chemical reaction, J. Korean Soc. Ind. Appl. Math, Vol. 21, 2017, 245–275.

G. S. Seth, B. Kumbhakar and R. Sharma: Unsteady hydromagnetic natural convection flow of heat-absorbing fluid within a

rotating vertical channel in a porous medium with Hall effect, J. Appl. Fluid Mech., Vol. 8, No. 4, 2015, 767–779.

M. Venkateswarlu, D. Venkata Lakshmi and G. Darmaiah: Influence of slip condition on radiative MHD flow of a viscous fluid in a parallel porous plate channel in presence of heat absorption and chemical reaction, J. Korean Soc. Ind. Appl. Math., Vol. 20, No. 4, 2016, 333–354.

G. S. Seth, R. Nandkeodyar and S. Md. Ansari: unsteady MHD convective flow within a parallel plate rotating channel with thermal source/sink in a porous medium under slip boundary conditions, Int. J. Eng. Sci. Technol, Vol. 2, No. 11, 2010, 1–16.

S. O. Adesanya and O. D. Makinde: MHD oscillatory slip flow and heat transfer in a channel filled with porous media, U.P.B. Sci. Bull., Series A, Vol. 76, No. 1, 2014, 197–204.